COMMUNICATIONS CHEMISTRY

ARTICLE

https://doi.org/10.1038/s42004-018-0094-z OPEN

Ring shape-dependent self-sorting of pillar[n]arenes assembled on a surface

Tomoki Ogoshi[1,2,3], Shu Takashima[1], Natsumi Inada[1], Hitoshi Asakawa[1,2,3], Takeshi Fukuma[1,2], Yoshiaki Shoji[4,5], Takashi Kajitani[4,5], Takanori Fukushima[4], Tomofumi Tada[6], Tomonori Dotera[7], Takahiro Kakuta[1,2] & Tada-aki Yamagishi[1]

Self-sorting, in which multiple components selectively assemble themselves by recognising self from others, is an attractive approach to produce supramolecular assemblies with controlled structures. Lock-and-key type complementary physical interactions are required for self-sorting because selective affinity is necessary to distinguish self from others. Here we show self-sorting behaviour based on a principle of geometrical complementarity by shape during our investigation of assembly of pentagonal pillar[5]arenes and hexagonal pillar[6]arenes on a surface. In the homoassembly systems, anionic pillar[5]arenes and pillar[6]arenes are adsorbed onto positively charged layers of cationic pillar[5]arenes and pillar[6]arenes, respectively, through cationic-anionic electrostatic interactions. In contrast, ionic pillar[5]arenes are adsorbed onto layers constructed from oppositely charged pillar[5]arenes, but ionic pillar[6]arenes are not. Equally, for the reverse combination, ionic pillar[6]arenes are adsorbed onto layers constructed from oppositely charged pillar[6]arenes, but ionic pillar[5]arenes are not. The geometrical complementarity by shape realises effective self-sorting even in non-directional multivalent ionic interactions.

[1] Graduate School of Natural Science and Technology, Kanazawa University, Kakuma-machi, Kanazawa 920-1192, Japan. [2] WPI Nano Life Science Institute, Kanazawa University, Kakuma-machi, Kanazawa 920-1192, Japan. [3] Japan Science and Technology Agency (JST), Precursory Research for Embryonic Science and Technology (PRESTO), 4-1-8 Honcho, Kawaguchi, Saitama 332-0012, Japan. [4] Laboratory for Chemistry and Life Science, Institute of Innovative Research, Tokyo Institute of Technology, 4259 Nagatsuta, Midori-ku, Yokohama 226-8503, Japan. [5] RIKEN SPring-8 Center, 1-1-1 Kouto, Sayo, Hyogo 679-5148, Japan. [6] Materials Research Center for Element Strategy, Department of Innovative and Engineered Materials, Tokyo Institute of Technology, Nagatsuta-cho, Midori-ku, Yokohama 226-8501, Japan. [7] Department of Physics, Kindai University, Kowakae 3-4-1, Higashi-Osaka 577-8502, Japan. Correspondence and requests for materials should be addressed to T.O. (email: ogoshi@se.kanazawa-u.ac.jp)

Self-sorting requires components to exhibit a higher affinity for themselves over other components, and is an attractive approach to produce supramolecular assemblies with controlled structures and creation of integrated functions[1–3]. Artificial self-sorting has been observed in certain molecular systems based on lock-and-key type complementary physical interactions such as hydrogen bonds[4,5], metal–ligand coordination bonds[6] and host–guest interactions[7–11]. Self-sorting is an attractive approach to produce complex supramolecular systems and materials; thus, self-sorting based on new principles is highly desired. For instance, the sequence of only four DNA bases defines the genetic code, which is of prime important for life. In a cell, different supramolecular assemblies acting independent functions were produced by the self-sorting of molecules. In this study, during our investigation of assembly of pillar[n]arenes on a surface, we discovered unexpected self-sorting behaviour dominated by the geometrical complementarity by shape of pillar[n]arenes. Pillar[n]arenes, which were first developed by our group in 2008[12], have highly symmetrical polygonal tubular structures; examples include pillar[5]arenes and pillar[6]arenes, which are pentagonal and hexagonal molecules, respectively[13–18]. Based on strong multivalent ionic interactions, we successfully constructed multilayer films with molecular-scale pores by consecutive adsorption of cationic and anionic pillar[5]arenes onto a solid substrate[19,20]. The distict tubular structure of the pillar[5]arenes and the presence of cationic and anionic groups at both edges of the pillar[5]arenes enabled the formation of multivalent ionic interactions and construction of multilayer film on a substrate.

Here we show self-sorting behaviour based on a principle of geometrical complementarity by shape during our investigation of assembly of pentagonal pillar[5]arenes and hexagonal pillar[6]arenes on a surface. The pillar[6]arene-based multilayer films are obtained by repeated alternating immersion in cationic and anionic pillar[6]arene solutions. We also examine assembly of ionic pillar[6]arenes onto layers constructed from oppositely charged pillar[5]arenes to fabricate multilayer films possessing different molecular-scale pores at desired positions. However, contrary to our expectations, assemblies form through cavity-shape-dependent self-sorting; ionic pillar[5]arenes are adsorbed onto layers constructed from oppositely charged pillar[5]arenes, but ionic pillar[6]arenes are not. Equally, for the reverse combination, ionic pillar[6]arenes are adsorbed onto layers constructed from oppositely charged pillar[6]arenes, but ionic pillar[5]arenes are not. The electrostatic cationic-anionic interactions used to form the assemblies are strong non-directional physical interactions, which means they are not inherently suitable for self-sorting. Nevertheless, the geometrical complementarity by shape realises the effective self-sorting. This behaviour is a consequence of the formation of different assembly patterns on the surface depending on the ring shape of the pillar[n]arenes.

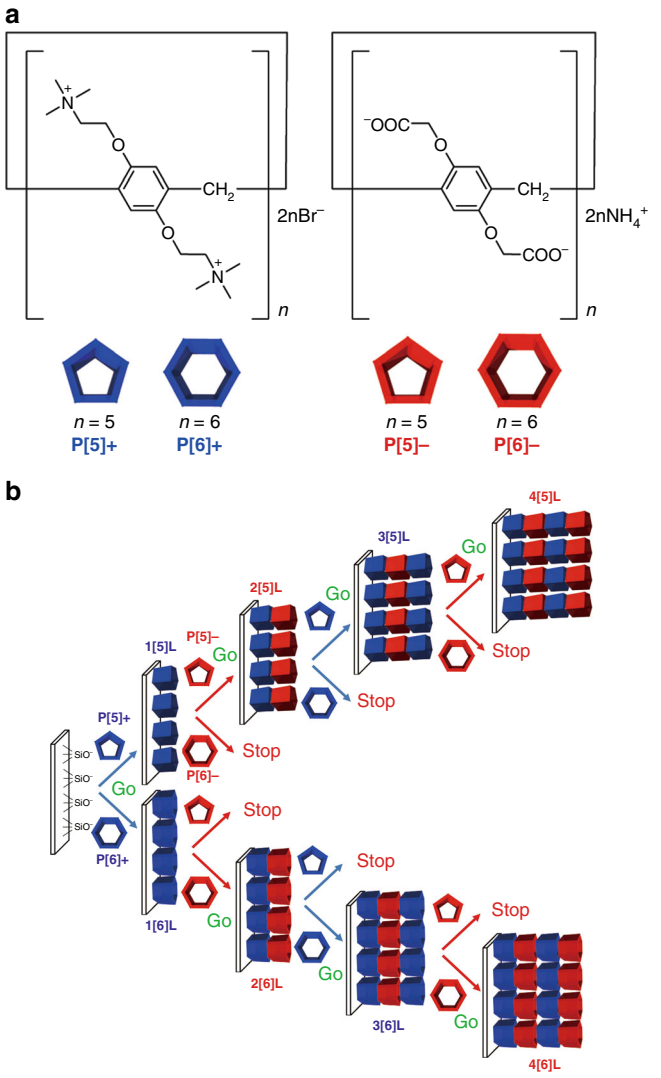

Fig. 1 Cavity-shape-dependent self-sorting on a surface. **a** Chemical structures of cationic (**P[5]**+) and anionic (**P[5]**−) pillar[5]arenes, and cationic (**P[6]**+) and anionic (**P[6]**−) pillar[6]arenes. **b** Multilayer films can be constructed using pillar[n]arenes with the same ring combinations, but cannot with the different ring combinations

Results

Cavity-shape-dependent self-sorting on a surface. Multilayer films of pillar[6]arenes ***n*[6]L** (***n*** is the number of deposited layers) were constructed by alternating adsorption of cationic pillar[6]arene (Fig. 1a, **P[6]** +)[21] and anionic pillar[6]arene (Fig. 1a, **P[6]**−)[22] on a quartz substrate.

This is the same approach that was used to construct multilayer pillar[5]arene films ***n*[5]L** from cationic pillar[5]arene (Fig. 1a, **P[5]**+)[23] and anionic pillar[5]arene (Fig. 1a, **P[5]**−)[24]. Each step in the construction of the multilayer assembly (Fig. 1b) was monitored by ultraviolet–visible (UV-vis) spectroscopy measurements.

The absorption at 293 nm, which corresponds to the absorption of 1,4-dialkoxybenzene units in pillar[6]arene, increased linearly with the number of deposited layers (Fig. 2a and b). The same trend was also observed for multilayer film constructed from **P[5]**+ and **P[5]**− (Supplementary Figure 1), and indicates that multilayer films were obtained by repeated alternating immersion in **P[6]**+ and **P[6]**− solutions. The rate of increase of the absorption intensity at 293 nm for the multilayer films of pillar[6]arenes was larger than that for the pillar[5]arenes (Fig. 2b), which suggests that the density of pillar[6]arenes on the substrate was higher than that of pillar[5]arenes. Hexagonal molecules can be closely packed to construct high-density supramolecular assemblies known as molecular tiling[25–28]. A possible reason for the higher density of pillar[6]arenes on the substrate compared with that of pillar[5]arenes is the higher symmetry of hexagonal pillar[6]arenes compared with that of pentagonal pillar[5]arenes.

To construct microporous films containing different pores, we investigated bilayer formation by adsorption of anionic **P[6]**− on **1[5]L**. Contrary to our expectations, an increase in absorption was not observed after immersing **1[5]L** with a cationic surface in

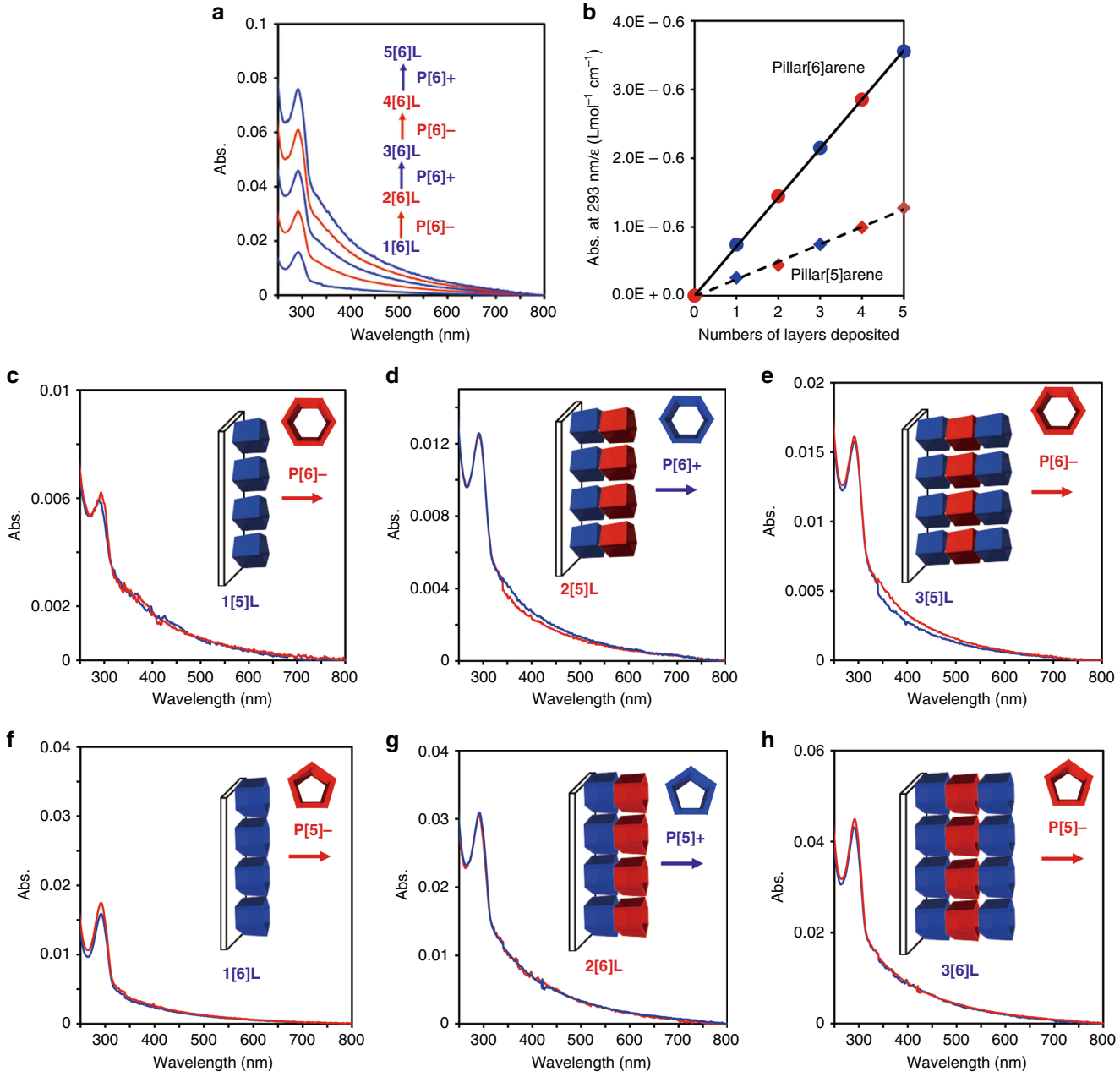

Fig. 2 UV-vis absorption spectra **a** UV-vis absorption spectra of the film obtained by consecutive adsorption of **P[6]**+ and **P[6]**−. **b** Plots of the absorbance/ε at 293 nm as a function of n for multilayers of ionic pillar[5]arenes (diamonds) and pillar[6]arenes (circles). UV-vis absorption spectra of **c** 1[5]L before (blue line) and after immersion in **P[6]**− (red line), **d 2[5]L** before (red line) and after immersion in **P[6]**+ (blue line), **e 3[5]L** before (blue line) and after immersion in **P[6]**− (red line), **f 1[6]L** before (blue line) and after immersion in **P[5]**− (red line), **g 2[6]L** before (red line) and after immersion in **P[5]**+ (blue line) and **h 3[6]L** before (blue line) and after immersion in **P[5]**− (red line)

anionic **P[6]**− in water (Fig. 2c), which indicates that **P[6]**− molecules were not adsorbed on the cationic monolayer **1[5]L**. Similarly, the absorption of the cationic **1[6]L** film did not change after immersing **1[6]L** in anionic **P[5]**− in water (Fig. 2f). As described above, multilayer films can be constructed using pillar[n]arenes with the same ring shape (Figs. 2a, b and Supplementary Figure 1); that is, homo-assembly of ionic pillar[5]arenes **P[5]**+ and **P[5]**− (Supplementary Figure 1) or ionic pillar[6]arenes **P[6]**+ and **P[6]**− (Fig. 2a). Thus, the assembly of ionic pillar[5]arenes and pillar[6]arenes on a surface was performed under ring shape-dependent self-sorting (Fig. 1b). We further investigated the ring shape-dependent self-sorting behaviour of the pillar[n]arenes using bilayer films of **2[5]L** and **2[6]L** with anionic charges. No increase in absorption was observed after immersing **2[5]L** film with anionic charges in cationic **P[6]**+ in water (Fig. 2d). The absorption of the **2[6]L** film with anionic charges also did not change after immersing **2[6]L** in cationic **P[5]**+ in water (Fig. 2g). The absorption of trilayer films **3[5]L** and **3[6]L** with cationic charges did not change after immersion in anionic **P[6]**− (Fig. 2e) and **P[5]**− (Fig. 2h), respectively, indicating that the ring shape-dependent self-sorting behaviour occurred regardless of the number of deposited layers (Fig. 1b).

Arrangement of cationic pillar[5,6]arenes on a surface. To better understand the reason why the ring shape-dependent self-sorting occurred on a substrate surface, we first investigated the molecular arrangement of ionic pillar[5]− and pillar[6]arenes on a surface by angle-dependent absorption measurements (Fig. 3a). Monolayer films **1[5]L** and **1[6]L** exhibited optical anisotropy. The absorbance at around 200 and 293 nm of monolayer films **1[5]L** and **1[6]L** was the highest when the angle of the incident UV light θ was perpendicular to the substrate surface and decreased as θ became shallower (Fig. 3b, c). Because time-dependent density functional theory (TD-DFT) calculations showed that the transition dipole moments of pillar[5]arenes and pillar[6]arenes are perpendicular to the longer molecular axis (Supplementary Figures 2 and 3), these observations indicate that the cationic pillar[n]arenes **P[5]**+ and **P[6]**+ were arranged perpendicular to the substrate through contact with one of the cationic edges of the molecule. This trend is the same as that observed for a two-dimensional (2D) hexagonal triptycene array on a substrate[28].

We directly investigated surface patterns of **1[5]L** and **1[6]L** by frequency modulation atomic force microscopy (FM-AFM) to reveal the reason for the ring shape-dependent self-sorting. Formation of pillar[5,6]arene assembly was also observed in mica surface for FM-AFM measurements. In the **1[6]L** film (Fig. 4f, g), hexagonal packing patterns were observed. However, the patterns did not display long-range structural order. As shown in Fig. 4g, the direction of the hexagonal packing pattern (yellow ring) indicated by blue line was different from that of another hexagonal packing pattern indicated by red line. The 2D fast Fourier transformation (FFT) spectrum (Fig. 4i) obtained from the FM-AFM image did not show a clear periodic contrast pattern with specific directionality, which also indicates that the hexagonal packing patterns did not exhibit long-range structural integrity.

Figure 4a and b show FM-AFM images of a **1[5]L** film. **1[5]L** showed different periodic patterns compared with those of the **1[6]L** film; hexagonal voids with regular periodicity were observed (Fig. 4a). The hexagonal voids (blue features) displayed high regularity and directionality over a long range (Fig. 4b). Clear 2D periodic contrasts with spacing of 2.3 nm were observed at 60° intervals in the FFT spectrum (Fig. 4d), which also indicates the long-range structural integrity of the hexagonal contrast patterns with voids produced by assembly of **P[5]**+ molecules. Overall, the **1[5]L** film showed hexagonal contrast patterns with voids with long-range structural integrity, whereas hexagonal patterns with short-range structural integrity were observed for the **1[6]L** film. These different patterns would contribute to the ring shape-dependent self-sorting of the pillar[n]arenes on the substrate surface. We also performed FM-AFM studies on the bilayer films of pillar[n]arenes (Supplementary Figure 4 and Supplementary Note 1).

To better understand the dependence of the pattern formation of the pillar[n]arenes on their ring shape, a Monte Carlo simulation was conducted considering **1[5]L** and **1[6]L** as regular pentagons or hexagons, respectively. In the simulation, an isotropic pair potential between the pentagons and hexagons consisting of an inner repulsive core and an outer thin attractive shell was originally used (Supplementary Figure 5 and Supplementary Note 2). We expected that **1[6]L** molecules might adopt regular hexagonal arrangement (i.e. triangular lattice); however, such regular arrangement was hardly realised (Fig. 4h) because of the dense packing of molecules, as indicated by the absorption intensity results (Fig. 2b). Indeed, we observed small hexagonal domains with random orientations, and thus the FFT spectrum of the molecules was circular as shown in the inset of Fig. 4j. We believe that the electrostatic repulsion force may hinder the growth of hexagonal domains for **1[6]L**. In contrast, **1[5]L** molecules adopted zig-zag arrangements or the partially regular arrangement of flattened hexagonal shapes (Fig. 4c), which exhibited Fourier peaks (Fig. 4e). Because of their pentagonal shape, the density of **1[5]L** molecules in the simulation was much lower than that of **1[6]L** without extra energetic cost. At the same time, the electrostatic repulsion force would contribute to the regular arrangement of the flattened hexagonal shapes.

The higher structural regularity of a monolayer film of pillar[5]arene **P[5]**+ than that of pillar[6]arene **P[6]**+ monolayer film was also observed for the multilayer films. Formation of pillar[5,6]arene assembly was also observed in silicon surface for

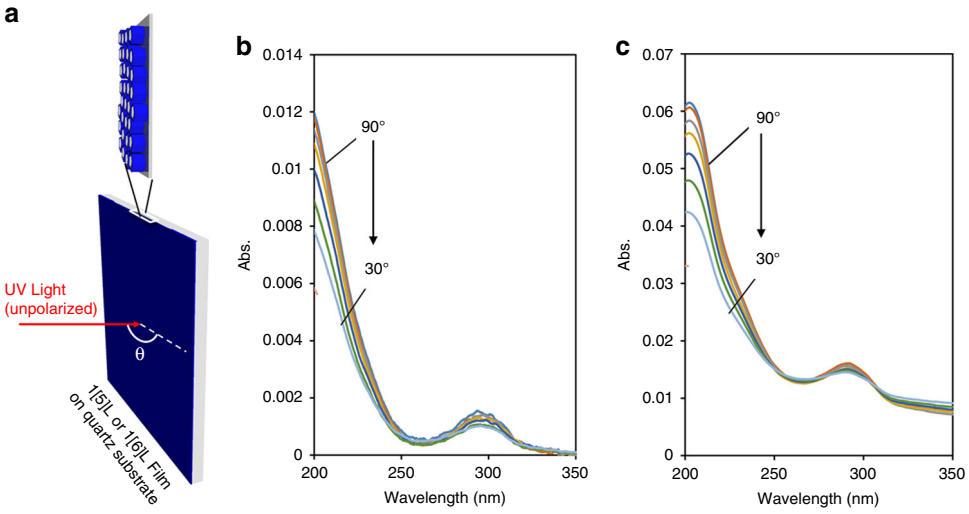

Fig. 3 Perpendicular arrangement of cationic pillar[5]− and pillar[6]arene molecules on a surface. **a** Schematic illustration of the experimental setup for the UV-vis absorption spectroscopy of monolayer **1[5]L** or **1[6]L** film on a quartz substrate. The angle of incident unpolarised UV light is represented by θ. **b**, **c** Anisotropic absorption properties of **1[5]L** and **1[6]L**. UV-vis absorption spectra of **1[5]L** and **1[6]L** on a quartz substrate measured during exposure to unpolarised UV light with various incident angles (θ of 30°, 40°, 50°, 60°, 70°, 80° and 90°). The downward arrows indicate incident angle change from 90° to 30°. The spectra were corrected for both the irradiated area and substrate absorption

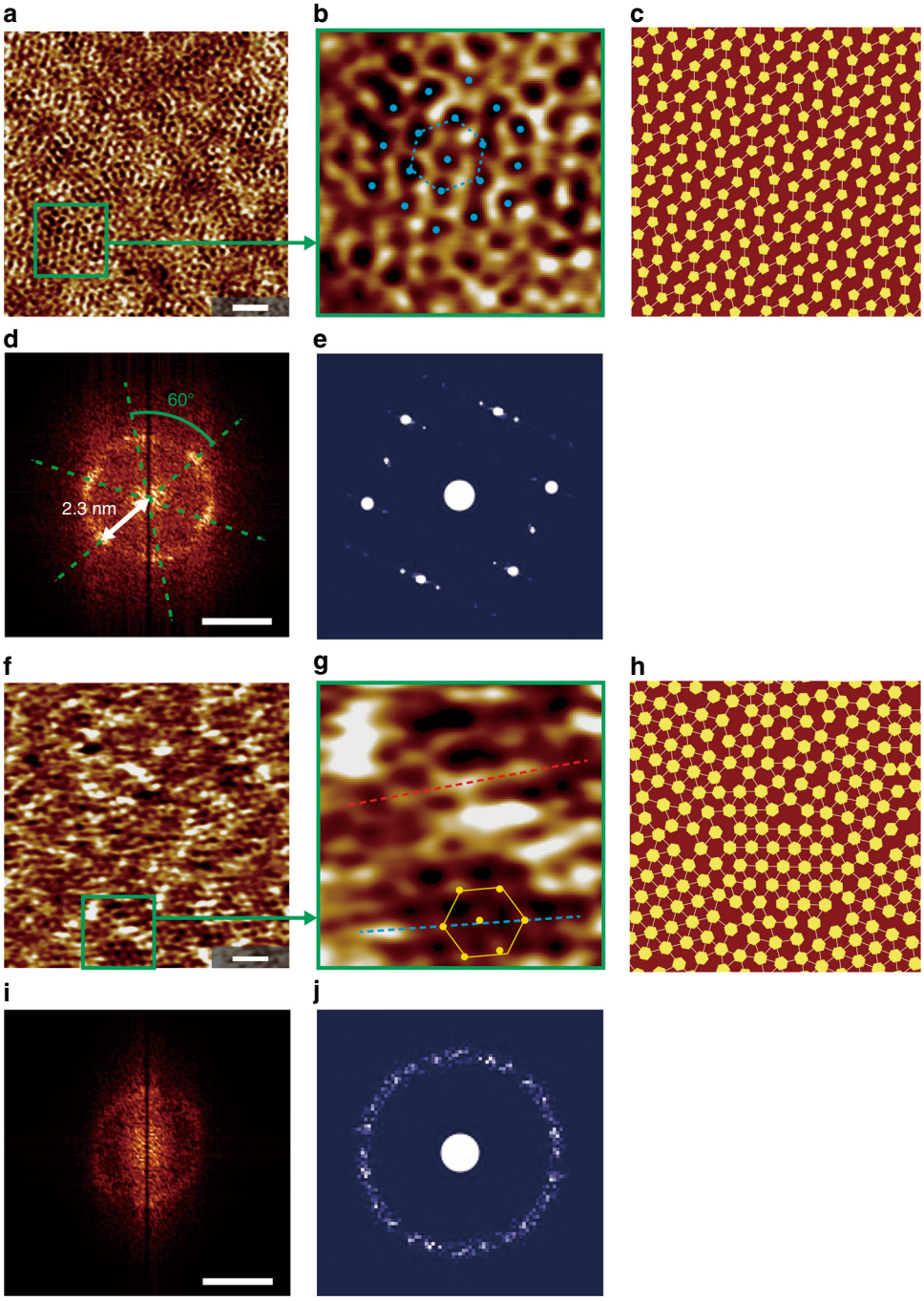

Fig. 4 Assembled structures of monolayer films constructed from ionic pillar[5]− and pillar[6]arenes. FM-AFM images of **a 1[5]L** and **f 1[6]L** Scale bar, 10 nm. **d**, **i** Fourier transform (FFT) spectra of FM-AFM images of **a 1[5]L** and **f 1[6]L**, respectively. Scale bar, 0.5 nm^{-1}. **b**, **g** Enlarged FM-AFM images of **a 1[5]L** and **f 1[6]L**, respectively. The blue features shown in (**b**) indicate that the hexagonal voids displayed high regularity and directionality over a long range. In contrast, in (**g**), the direction of the hexagonal packing (the yellow ring) pattern indicated by blue line was different from that of another hexagonal packing pattern indicated by red line. **c** Snapshot of a portion of a 1000-molecule **1[5]L** system with a packing fraction η of 0.224 and **e** the corresponding FFT image. **h** Snapshot of a portion of the 1000-molecule **1[6]L** system with η = 0.294, and **j** the corresponding FFT image

GI-XRD measurements. Grazing-incidence X-ray diffraction (GI-XRD) measurements revealed that the multilayer film **11[5]L** prepared by alternating adsorption of ionic pillar[5]arenes **P[5]+** and **P[5]−** showed a diffraction spot ($d = 9.2$ Å) in the out-of-plane direction (Fig. 5a).

This diffraction was considered to result from the layered structure of pillar[5]arenes because the d value corresponds to the length of a pillar[5]arene molecule (ca. 8–9 Å)[16]. The layers assembled parallel to the substrate surface. The long-range structural integrity observed for **1[5]L** should result in long-range parallel assembly of the layers to the substrate. In contrast, a diffraction spot in the out-of-plane direction was not observed for the multilayer film **11[6]L** (Fig. 5b), prepared by alternating adsorption of ionic pillar[6]arenes **P[6]+** and **P[6]−**. This indicates the low structural regularity of the multilayer films constructed from **P[6]+** and **P[6]−**.

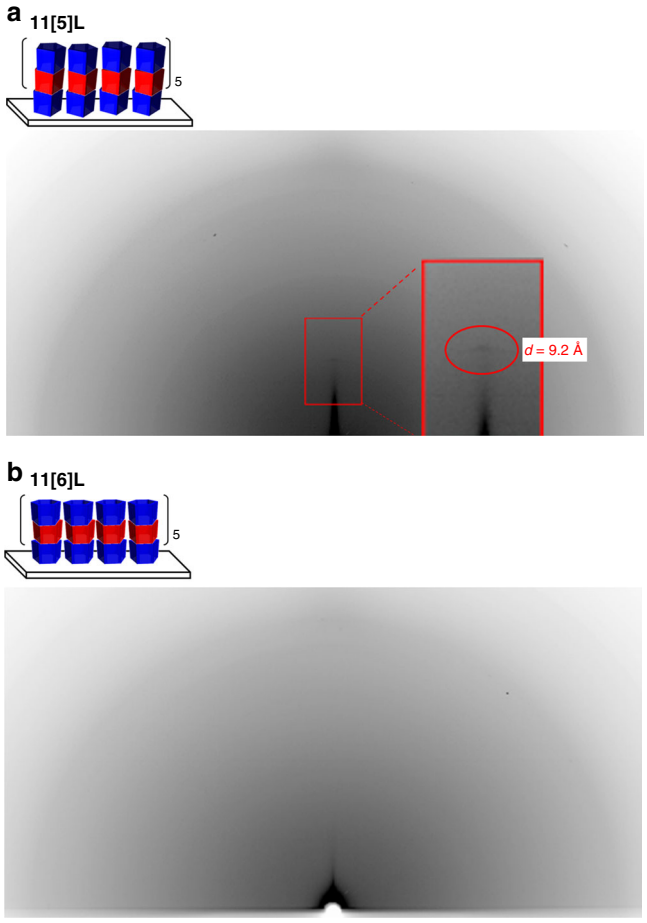

Fig. 5 Assembled structures of multilayer films constructed from ionic pillar[5]− and pillar[6]arenes. GI-XRD images of **a 11[5]L** and **b 11[6]L** on a silicon wafer. Pictures of **11[5]L** and **11[6]L** is provided. The red square is enlarged GI-XRD image. A diffraction spot ($d = 9.2$ Å) in the out-of-plane direction was observed in the red circle

Discussion

We discovered self-sorting behaviour when we investigated the assembly of ionic pillar[n]arenes on a surface. The self-sorting on a surface is based on the principle of geometrical complementarity by shape. The lattice difference resulting from the shape different between pentagonal and hexagonal structures should contribute to the self-sorting. The self-sorting observed here is of interest because it is accomplished by match and mismatch of the ring shape of pillar[n]arenes. The ultimate challenge will be to propagate cavity-shape information on the surface to provide shape-recognisable adsorption and adhesive materials.

Methods

UV-vis measurements. UV-vis absorption spectra were recorded with a JASCO V-670 spectrometer. quartz substrates (width: 4 mm, length 10 mm) were used for the UV-vis measurements in the film states.

Anisotropic UV-vis absorption measurements. The incident angle-dependent changes in the absorption spectra of the films were measured by a JASCO model V-670 spectrometer using a rotary sample holder (RSH-744). Anisotropic UV-vis absorption spectra of monolayer films **1[5]L** and **1[6]L** on a quartz substrate, measured upon exposure to un-polarized UV light with various incident angles (θ of 30°, 40°, 50°, 60°, 70°, 80° and 90°). The spectra were corrected for both the irradiated area and the contribution of the absorption of the substrate.

FM-AFM measurements. Aqueous solution of **P[5]**+ or **P[6]**+ (0.1 wt%) was deposited onto a freshly cleaved mica substrate (Grade V1, SPI Supplies). The sample was incubated at room temperature for 2 h and rinsed with Milli-Q water to remove unadsorbed ionic pillar[n]arenes. FM-AFM measurements were performed using a home-built low-noise deflection sensor and a photothermal excitation system[29] with commercially available AFM controllers (ARC2, Asylum research and Nanonis OC4, SPECS). All AFM experiments were performed in MilliQ water with a commercially available silicon cantilever (PPP-NCHAuD, Nanoworld). The obtained FM-AFM images were processed using Gwyddion software.

Synchrotron radiation X-ray diffraction experiments. The grazing-incidence X-ray diffraction (GI-XRD) images of thin-films of **11[5]L** and **11[6]L** were obtained using the BL45XU beamline at SPring-8 (Hyogo, Japan) equipped with a Pilatus3X 2M (Dectris) detector. The scattering vector, $q = 4\pi\sin\theta/\lambda$, and the position of the incident X-ray beam on the detector were calibrated using several orders of layer reflections from silver behenate ($d = 58.380$ Å), where 2θ and λ refer to the scattering angle and wavelength of the X-ray beam (1.0 Å), respectively. The sample-to-detector distance was 0.34 m. The obtained diffraction images were integrated along the Debye-Scherrer ring to afford one-dimensional (1D) intensity data using the software FIT2D (http://www.esrf.eu/computing/scientific/FIT2D/).

Theoretical calculations. All the DFT calculations were performed using Gaussian 09 program package. The ground-state geometry of pillar[5]arene with 10 ethoxy moieties and pillar[6]arene with 12 ethoxy moieties were fully optimized by the M06-2X/6-31G(d,p) level of calculation and was confirmed by harmonic vibrational frequency analyses. To estimate excited states and transition dipole moments, we performed time-dependent DFT (TD-DFT) calculations at the optimized geometry [M06-2X/6-31G(d,p)] by using M06 functional and 6-311G(d,p) basis set.

Pre-treatment of substrates. Quartz substrates were sonicated in concentrated nitric acid for 30 min and finally washed with methanol for three times, and dried for 12 h at 100 °C to generate anionic silanol moieties on the surface. For FM-AFM and GI-XRD measurements, freshly cleaved mica and silicon wafer were used as substrates, respectively.

Formation of assembly of pillar[5,6]arenes on surface. The homo-assembly of **P[5]**+ and **P[5]**− was previously investigated by us[19]. We applied the same assembly condition for homo-assembly using **P[6]**+ and **P[6]**− on a quartz surface as follows. The substrate was immersed in **P[m]**+ in aqueous solution (1 wt%) to introduce **P[m]**+ molecules onto the anionic substrate surface. In the case of **P[5]**+, an immersion time of 2 h was long enough to reach equilibrium state. In the case of **P[6]**+, immersion for 8 h was required to reach equilibrium state. The sample was washed with a large amount of water to remove excess unadsorbed **P[m]**+ molecules and then dried for 2 h at 25 °C under reduced pressure to obtain a cationic monolayer (**1[m]L**). Then, **1[m]L** was immersed in **P[m]**− in aqueous solution (1 wt%) (2 and 8 h were required to reach equilibrium state for **P[5]**− and **P[6]**−, respectively) to introduce **P[m]**− molecules onto **1[m]L**. Each sample was washed with a large amount of water and dried under vacuum for 2 h at 25 °C to give a bilayer with an anionic surface (**2[m]L**). Multilayer films (**n[m]L**) were obtained by repeating the alternating immersion steps in **P[m]**+ and **P[m]**− solutions. The construction of the multilayers was monitored after each immersion step with a UV-vis spectrometer (Fig. 2a and Supplementary Figure 1).

We applied the same assembly condition[19] for co-assembly using ionic pillar[5]− and pillar[6]arenes on **n[6]L** and **n[5]L** films as follows. An **n[5]L** or **n[6]L** film with a cationic surface (**n** = 1 or 3) was immersed in **P[6]**− or **P[5]**− aqueous solution (1 wt%) for 8 h, respectively, and then washed with a large amount of water and dried under vacuum for 2 h at 25 °C. A **2[5]L** or **2[6]L** film with an anionic surface was immersed in **P[6]**+ or **P[5]**+ aqueous solution (1 wt%) for 8 h, respectively, and then washed with a large amount of water and dried under vacuum for 2 h at 25 °C.

Simulation. We assume that molecules are densely distributed on mica substrates, and that the number of molecules (N) is constant due to their electrostatic absorption potentials. We therefore used NVT Monte Carlo simulations of $N = 1000$ molecules confined to a square box of area A with periodic boundary conditions; the packing fraction of molecules is defined by $\eta = S / A$, where S is the area of polygonal shapes. Starting from a random state, all runs are consisted of a quenching at a reduced temperature $kBT/\varepsilon \cong 0.3$. The typical number of Monte Carlo steps was between 10^8 and 2×10^8 as appropriate.

Data availability

The data supporting the findings of this study are available within the article and its Supplementary Information files. All other relevant source data are available from the corresponding author upon reasonable request.

Received: 6 August 2018 Accepted: 16 November 2018
Published online: 07 December 2018

References

1. Safont-Sempere, M. M., Fernández, G. & Würthner, F. Self-sorting phenomena in complex supramolecular systems. *Chem. Rev.* **111**, 5784–5814 (2011).
2. Jędrzejewska, H. & Szumna, A. Making a right or left choice: chiral self-sorting as a tool for the formation of discrete complex structures. *Chem. Rev.* **117**, 4863–4899 (2017).
3. Nitschke, J. R. Construction, substitution, and sorting of metallo-organic structures via subcomponent self-assembly. *Acc. Chem. Res.* **40**, 103–112 (2007).
4. Wu, A. & Isaacs, L. Self-sorting: the exception or the rule? *J. Am. Chem. Soc.* **125**, 4831–4835 (2003).
5. Onogi, S. et al. In situ real-time imaging of self-sorted supramolecular nanofibres. *Nat. Chem.* **8**, 743–752 (2016).
6. Bloch, W. M. & Clever, G. H. Integrative self-sorting of coordination cages based on 'naked' metal ions. *Chem. Commun.* **53**, 8506–8516 (2017).
7. Tomimasu, N., Kanaya, A., Takashima, Y., Yamaguchi, H. & Harada, A. Social self-sorting: alternating supramolecular oligomer consisting of isomers. *J. Am. Chem. Soc.* **131**, 12339–12343 (2009).
8. Talotta, C., Gaeta, C., Qi, Z., Schalley, C. A. & Neri, P. Pseudorotaxanes with self-sorted sequence and stereochemical orientation. *Angew. Chem. Int. Ed.* **52**, 7437–7441 (2013).
9. He, Z., Jiang, W. & Schalley, C. A. Integrative self-sorting: a versatile strategy for the construction of complex supramolecular architecture. *Chem. Soc. Rev.* **44**, 779–789 (2015).
10. Neal, E. A. & Goldup, S. M. A kinetic self-sorting approach to heterocircuit [3] rotaxanes. *Angew. Chem. Int. Ed.* **55**, 12488–12493 (2016).
11. Taisuke, M., Sota, S., Atsutoshi, Y., Sho, K. & Hiroyuki, I. Self-sorting of two hydrocarbon receptors with one carbonaceous ligand. *Angew. Chem. Int. Ed.* **55**, 15339–15343 (2016).
12. Ogoshi, T., Kanai, S., Fujinami, S., Yamagishi, T. & Nakamoto, Y. para-Bridged symmetrical pillar[5]arenes: their Lewis acid catalyzed synthesis and host-guest property. *J. Am. Chem. Soc.* **130**, 5022–5023 (2008).
13. Ogoshi, T., Yamagishi, T. & Nakamoto, Y. Pillar-shaped macrocyclic hosts pillar[n]arenes: new key players for supramolecular chemistry. *Chem. Rev.* **116**, 7937–8002 (2016).
14. Ogoshi, T., Kakuta, T. & Yamagishi, T. Applications of pillar[n]arene-based supramolecular assemblies. *Angew. Chem. Int. Ed*. https://doi.org/10.1002/anie.201805884 (2018).
15. Kakuta, T., Yamagishi, T. & Ogoshi, T. Stimuli-responsive supramolecular assemblies constructed from pillar[n]arenes. *Acc. Chem. Res.* **51**, 1656–1666 (2018).
16. Xue, M., Yang, Y., Chi, X. D., Zhang, Z. B. & Huang, F. H. Pillararenes, a new class of macrocycles for supramolecular chemistry. *Acc. Chem. Res.* **45**, 1294–1308 (2012).
17. Strutt, N. L., Zhang, H. C., Schneebeli, S. T. & Stoddart, J. F. Functionalizing pillar[n]arenes. *Acc. Chem. Res.* **47**, 2631–2642 (2014).
18. Ogoshi, T. (ed) *Pillararenes, Monographs in Supramolecular Chemistry No. 18* (The Royal Society of Chemistry, London, 2016).
19. Ogoshi, T., Takashima, S. & Yamagishi, T. Molecular recognition with microporous multilayer films prepared by layer-by-layer assembly of pillar[5] arenes. *J. Am. Chem. Soc.* **137**, 10962–10964 (2015).
20. Ogoshi, T., Takashima, S. & Yamagishi, T. Photocontrolled reversible guest uptake, storage, and release by azobenzene-modified microporous multilayer films of pillar[5]arenes. *J. Am. Chem. Soc.* **140**, 1544–1548 (2018).
21. Yu, G., Zhou, J., Shen, J., Tang, G. & Huang, F. Cationic pillar[6]arene/ATP host-guest recognition: selectivity, inhibition of ATP hydrolysis, and application in multidrug resistance treatment. *Chem. Sci.* **7**, 4073–4078 (2016).
22. Yu, G. et al. A water-soluble pillar[6]arene: synthesis, host-guest chemistry, and its application in dispersion of multiwalled carbon nanotubes in water. *J. Am. Chem. Soc.* **134**, 13248–13251 (2012).
23. Ma, Y. J. et al. A cationic water-soluble pillar[5]arene: synthesis and host-guest complexation with sodium 1-octanesulfonate. *Chem. Commun.* **47**, 12340–12342 (2011).
24. Ogoshi, T., Hashizume, M., Yamagishi, T. & Nakamoto, Y. Synthesis, conformational and host-guest properties of water-soluble pillar[5]arene. *Chem. Commun.* **46**, 3708–3710 (2010).
25. Blunt, M. O. et al. Random tiling and topological defects in a two-dimensional molecular network. *Science* **322**, 1077–1081 (2008).
26. Tahara, K., Lei, S., Adisoejoso, J., De Feyter, S. & Tobe, Y. Supramolecular surface-confined architectures created by self-assembly of triangular phenylene-ethynylene macrocycles via van der Waals interaction. *Chem. Commun.* **46**, 8507–8525 (2010).
27. Ogoshi, T., Yoshikoshi, K., Sueto, R., Nishihara, H. & Yamagishi, T. Porous carbon fibers containing pores with sizes controlled at the angstrom level by the cavity size of pillar[6]arene. *Angew. Chem. Int. Ed.* **54**, 6466–6469 (2015).
28. Seiki, N. et al. Rational synthesis of organic thin films with exceptional long-range structural integrity. *Science* **348**, 1122–1126 (2015).
29. Fukuma, T. Wideband low-noise optical beam deflection sensor with photothermal excitation for liquid-environment atomic force microscopy. *Rev. Sci. Instrum.* **80**, 023707 (2009).

Acknowledgements

This work was partially supported by Grants-in-Aid for Scientific Research (B) (JP16H04130 for T.O and JP16H04037 for T.D.) for Scientific Research on Innovative Areas (2601): π-System Figuration (JP15H00990 for T.O., JP26102017 for T.T. and JP26102008 for Taka.F.) and the 'Dynamic Alliance for Open Innovation Bridging Human, Environment and Materials' from the Ministry of Education, Culture, Sports, Science, and Technology (MEXT), Japan, JST PRESTO Grant Number (JPMJPR1313 for T.O., JPMJPR1411 for H.A.), JST CREST Grant Number (JPMJCR18R3 for T.O.) and Kanazawa University CHOZEN Project. The synchrotron GI-XRD experiments were performed at the BL45XU in the SPring-8 with the approval of the RIKEN SPring-8 (proposal no. 20160027). NanoLSI is supported by the World Premier International Research Center (WPI) Initiative, Japan.

Author contributions

T.O. conceived the project and designed the experiments. T.O., S.T., Takah.K. and T.-a.Y. synthesised the ionic pillar[5]arenes and pillar[6]arenes and constructed the mono- and multilayer films. N.I., H.A. and Take.F. performed the FM-AFM measurements and analysed the surface images of the hexagonal packing and void formation. Y.S., Takas.K., and Taka.F. carried out the anisotropic absorption and GI-XRD measurements. T.D. performed the simulations of the formation of the hexagonal packing and void formation, and T.O. and T.T. performed the DFT calculations. All authors analysed and discussed the results, and co-wrote the paper.

Additional information

Supplementary information accompanies this paper at https://doi.org/10.1038/s42004-018-0094-z.

Competing interests: The authors declare no competing interests.

Reprints and permission information is available online at http://npg.nature.com/reprintsandpermissions/

Publisher's note: Springer Nature remains neutral with regard to jurisdictional claims in published maps and institutional affiliations.